Article

Hydroxyurea Induces Hydroxyl Radical-Mediated Cell Death in *Escherichia coli*

Bryan W. Davies,[1] Michael A. Kohanski,[3,4] Lyle A. Simmons,[1,6,7] Jonathan A. Winkler,[5,7] James J. Collins,[2,4] and Graham C. Walker[1],*

[1]Department of Biology, Massachusetts Institute of Technology, Cambridge, MA 02139, USA
[2]Howard Hughes Medical Institute, Department of Biomedical Engineering, Center for BioDynamics, and Center for Advanced Biotechnology
[3]Department of Biomedical Engineering and Center for BioDynamics
[4]Boston University School of Medicine
[5]Program in Molecular Biology, Cell Biology, and Biochemistry
Boston University, Boston, MA, USA
[6]Department of Molecular, Cellular, and Developmental Biology, University of Michigan, Ann Arbor, MI 48109, USA
[7]These authors contributed equally to this work
*Correspondence: gwalker@mit.edu
DOI 10.1016/j.molcel.2009.11.024

SUMMARY

Hydroxyurea (HU) specifically inhibits class I ribonucleotide reductase (RNR), depleting dNTP pools and leading to replication fork arrest. Although HU inhibition of RNR is well recognized, the mechanism by which it leads to cell death remains unknown. To investigate the mechanism of HU-induced cell death, we used a systems-level approach to determine the genomic and physiological responses of *E. coli* to HU treatment. Our results suggest a model by which HU treatment rapidly induces a set of protective responses to manage genomic instability. Continued HU stress activates iron uptake and toxins MazF and RelE, whose activity causes the synthesis of incompletely translated proteins and stimulation of envelope stress responses. These effects alter the properties of one of the cell's terminal cytochrome oxidases, causing an increase in superoxide production. The increased superoxide production, together with the increased iron uptake, fuels the formation of hydroxyl radicals that contribute to HU-induced cell death.

INTRODUCTION

Hydroxyurea (HU) is commonly used in both prokaryotes and eukaryotes to study DNA damage-independent replication fork arrest (Lopes et al., 2001; Sogo et al., 2002; Timson, 1975). HU is exquisitely specific for inhibiting class I ribonucleotide reductase (RNR), the enzyme responsible for the synthesis of dNTPs under aerobic conditions in many organisms, including *Escherichia coli*, yeast, and humans (Rosenkranz et al., 1967; Sinha and Snustad, 1972). Several lines of evidence have indicated that RNR is the primary, if not only, cellular target of HU (Fuchs and Karlstrom, 1973; Kren and Fuchs, 1987; Sjoberg et al., 1986; Sneeden and Loeb, 2004). Depletion of dNTP pools through HU treatment leads to replication fork arrest and subsequent

genomic instability (Ahmad et al., 1998; Nakayama et al., 1994), most likely through substrate starvation (Foti et al., 2005; Godoy et al., 2006; Timson, 1975). Although HU has been used to study replication fork arrest for decades, very little is known about the downstream physiological effects of HU-dependent replication fork arrest, especially the mechanism by which HU leads to loss of cell viability and eventual lysis.

An intriguing but unexplained observation is that prolonged HU stress results in cell death and lysis mediated in part by the *mazEF* and *relBE* toxin/antitoxin modules (Godoy et al., 2006). Depletion of thymine pools (thymineless death) has similarly been suggested to involve MazF activation in *E. coli* (Sat et al., 2003). Our observation that variants of the translesion DNA polymerase UmuC, acting in combination with the translesion polymerase DinB and the *umuD* gene products, may mitigate such *mazEF*- or *relBE*-induced death has led us to suggest that HU-induced death of *E. coli* is brought about not by stalled replication forks directly, but rather through a series of downstream processes involving the toxin/antitoxin pairs *mazEF* and *relBE* (Godoy et al., 2006).

To understand how HU-dependent replication fork arrest leads to cell death, we used a systems-level analysis to identify the genomic and physiological effects of HU treatment. We present a mechanism whereby HU treatment rapidly induces several survival responses, including upregulation of the SOS response, downregulation of cell division inhibition, and induction of RNR synthesis. However, as HU stress continues, toxin modules MazF and RelE are activated, triggering a cascade of events that eventually results in the production of deleteriously hydroxyl radicals. The production of hydroxyl radicals is exacerbated by increased iron uptake, and these harmful reactive oxygen species contribute to the majority of HU-mediated cell death in *E. coli*.

RESULTS

Genome-wide Analysis Defines Transcriptional Perturbations Induced by HU Treatment

When exponentially growing *E. coli* strain MC4100 is treated with 100 mM HU in liquid culture, cell growth quickly ceases.

However, cells do not begin to die until 2–3 hr into the treatment, and cell survival declines to ~0.1% by 6 hr (Figure 1). We examined gene expression profiles of exponentially growing MC4100 cultures following 1 hr of treatment with or without 100 mM HU. At this 1 hr time point, HU-treated cultures do not show decreased survival but do show growth inhibition (Figure 1A). We hypothesized that expression profiles at this time during HU treatment would allow us to gain insights into the early cellular events that lead to cell death and lysis.

RNA from three independent cultures treated with or without HU were analyzed using Affymetrix Antisense Genome microarrays. The expression results were integrated into an *E. coli* microarray expression database (Faith et al., 2007; http://m3d. bu.edu/) for analysis comparing the HU results to more than 500 additional expression profiles (Faith et al., 2007). We examined significance (z score) of gene expression on a gene-by-gene basis through comparison of expression levels with or without HU treatment in the framework of the mean and standard deviation (SD) of expression for each gene across all conditions in the compendium (see Experimental Procedures for additional details). This allowed us to determine the statistically significant changes in expression due to HU treatment in terms of units of SD by subtracting, on a gene-by-gene basis, the z score for an untreated control from the z score for an HU-treated sample. This procedure allowed us to filter our expression profile to identify those genes that showed altered transcript level specifically in response to HU (Table S1 available online).

HU Rapidly Induces Survival Responses to Manage DNA Damage

Our microarray analysis showed induction of cell survival responses to manage HU-induced cell stress (Table S1). We have grouped these survival responses into three categories (Table 1).

(1) Upregulation of Ribonucleotide Reductase Synthesis

Consistent with previous observations (Gibert et al., 1990), we found a significant increase in gene and protein expression of the components of class I RNR, NrdA and NrdB, in response to HU treatment (Table 1 and Figures S1A and S1B). In addition, genes encoding *E. coli* anaerobic class III RNR (*nrdDG*) and a cryptic RNR (*nrdEF*) (Jordan and Reichard, 1998) showed significant transcriptional increases (Table 1). We were surprised to find substantial induction of *nrdDG*, given that any NrdDG produced would be irreversibly inactivated under our aerobic conditions. These observations suggest that upregulation of all RNR genes in response to HU-induced dNTP pool depletion is a strong survival response.

(2) Upregulation of Primosome Components

We also observed that components of the primosome, PriA and PriB, were substantially upregulated by HU treatment (Table 1). PriA and PriB can assemble forks on either the leading or lagging strand (Heller and Marians, 2005, 2006; Lovett, 2005). The PriA pathway for replication restart is most efficient on fork structures without gaps in the leading strand. This structure could be formed after the collapse of a replication fork. An alternative PriC-dependent pathway preferentially utilizes forks with large gaps in the leading strand. We did not observe upregulation of *priC* (Table 1), an observation consistent with the mode of fork damage induced by HU treatment. Upregulation of primosome components may help restart replication forks stalled or collapsed following HU treatment. Of note, induction of primosome components is not part of the SOS response (Simmons et al., 2008a).

(3) Activation of the SOS Response

Consistent with previous work (Barbe et al., 1987), our microarray analysis revealed that numerous genes in the DNA-damage-responsive SOS network were induced by HU treatment (Table 1). The SOS response involves the upregulation of 57 genes involved in numerous aspects of DNA repair and other cellular functions (Simmons et al., 2008a). In agreement with the transcriptional data, SulA and RecA protein levels showed a significant increase following HU challenge (Figures S1C and S1D).

Recent work has shown that a small subpopulation of cells can account for large transcriptional changes in microarray analyses of the SOS response (Britton et al., 2007; Simmons et al., 2008b). To determine the population of SOS-induced cells after HU treatment, we used the pL(*lexO*)-GFP construct in which GFP expression is controlled by LexA (Dwyer et al., 2007) as a single-cell marker of SOS induction. No GFP fluorescence was observed in the absence of HU (data not shown), but we did observe GFP fluorescence soon after HU treatment (Figure 1B, i). After a 30 min exposure to HU, GFP fluorescence was clearly visible in the vast majority of cells (Figure 1B, ii), indicating that SOS induction occurred uniformly in the bulk of the population.

To explore the contribution of the SOS response to HU survival, we tested the sensitivity of the *lexA3* mutant strain to increasing amounts of HU (Figure 1C). The *lexA3* strain carries a noncleavable form of LexA, effectively preventing SOS induction (Friedberg et al., 2005; Mount et al., 1972). The *lexA3* strain was ~10-fold more sensitive relative to the parental strain through a range of HU concentrations, indicating that activation of the SOS-regulated genes helps cells survive HU exposure. HU is much less stable in liquid culture than in solid LB agar (S.T. Lovett, personal communication), possibly due to increased oxidation of HU in liquid. We found that 100 mM HU was required for significant killing in liquid cultures (Figure 1A), whereas 5–30 mM HU was sufficient to observe growth difference between strains in LB agar plating assays (Figure 1C).

HU treatment induces extreme filamentation (Godoy et al., 2006), which could occur due to SulA-mediated inhibition of septum formation. However, upregulation of SulA alone cannot completely account for the observed increase in filamentation because HU-induced filamentation still occurs in a Δ*sulA* background (Figure S1E and S1F). A functionally linked cluster of genes involved early in cell division, including several genes involved in septum formation (e.g., *ftsZ*, *ftsQ*, *zipA*) and a positive regulator of *ftsZ*, *rcsB* (Table 1), showed significant downregulation in our microarrays. In agreement with the transcriptional result, we observed a decrease in FtsZ protein level (Figure S1G). To determine whether the downregulation of genes required for septum assembly was sufficient to perturb septum formation, we analyzed Z ring formation at the single-cell level using an *ftsZ*-GFP fusion (Weiss et al., 1999). FtsZ-GFP does not functionally complement endogenous FtsZ but is able to decorate the wild-type protein forming Z rings, allowing for visualization by
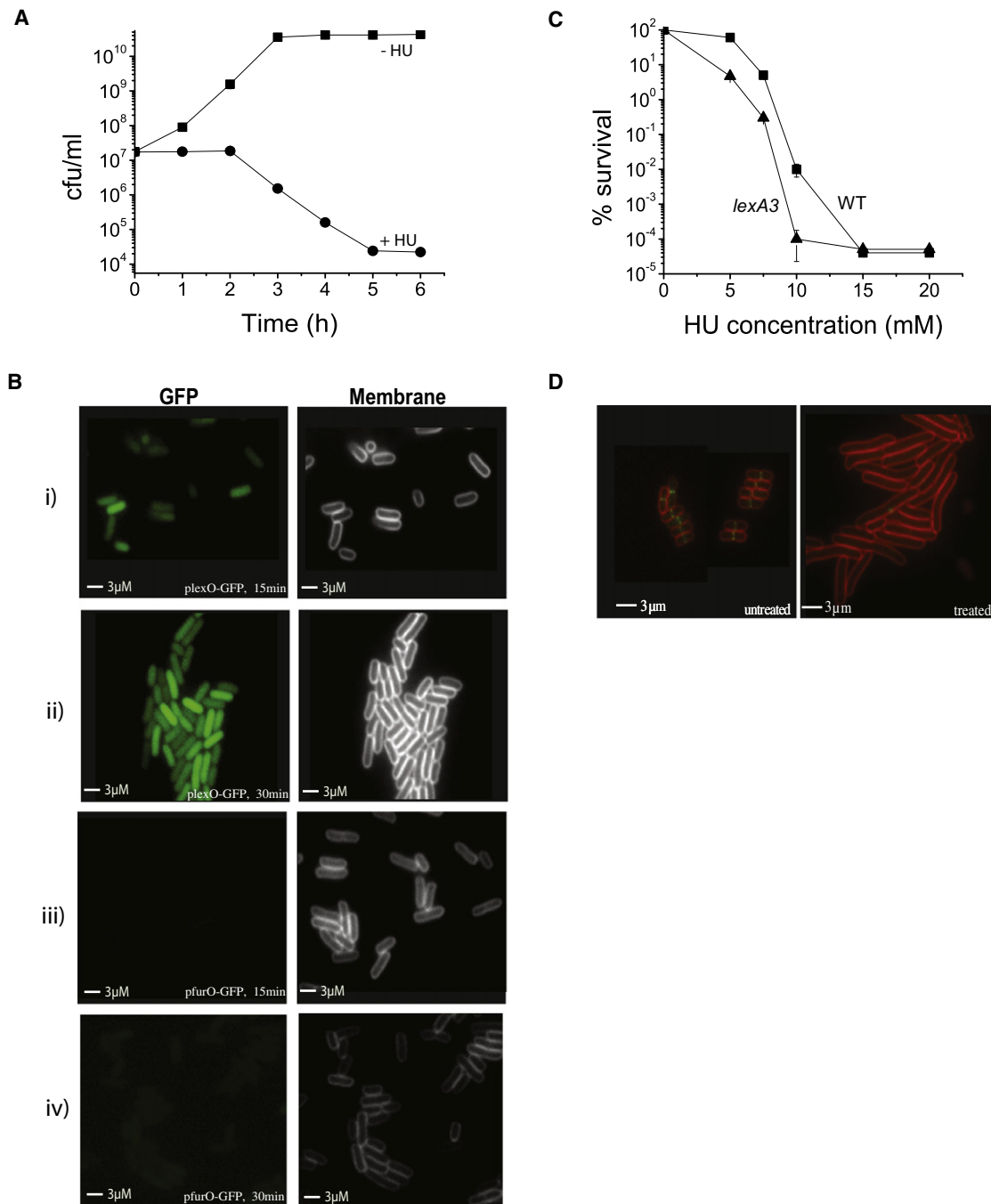
Figure 1. HU Treatment Induces DNA Damage Responses

(A) Survival of exponentially growing MC4100 cultures treated with (●) or without (■) 100 mM HU for the indicated times.

(B) MC4100 pL(*lexO*)-GFP treated with 100 mM HU for 15 min (i) and 30 min (ii). MC4100 pL(*lexO*)-GFP did not show GFP fluorescence in the absence of HU (data not shown). MC4100 pL(*furO*)-GFP treated with 100 mM HU for 15 min (iii) and 30 min (iv). MC4100 pL(*furO*)-GFP did not show GFP fluorescence in the absence of HU (data not shown).

(C) WT AB1157 (■) and AB1157 *lexA3* (■) were spotted on LB agar plates containing increasing concentrations of HU.

(D) MC4100 carrying P$_{lac}$*ftsZ*-GFP treated with 2.0 μM IPTG with or without 100 mM HU for 1 hr.

Each data point represents the average of at least three independent experiments, and the error bars represent the standard error of the independent measurements.

Table 1. Functional Groups of Differentially Regulated Genes Identified by Microarray Analysis Having a Biologically Relevant Effect on the *E. coli* Cellular Response to HU

Gene	Gene Product/Function	Z Score ± SE[1] (+HU vs. −HU)
	Ribonucleotide Reductases	
nrdA	subunit A class I ribonucleotide reductase	+1.82 ± 0.15
nrdB	subunit B class I ribonucleotide reductase	+2.52 ± 0.14
nrdD	class III ribonucleotide reductase, anaerobic	+2.25 ± 0.25
nrdG	NrdD activating enzyme	+2.38 ± 0.20
nrdH	electron transport system for NrdEF	+2.32 ± 0.09
nrdI	part of *nrdHIEF* operon; function unknown	+2.53 ± 0.09
nrdE	subunit α cryptic class I ribonucleotide reductase	+2.33 ± 0.05
nrdF	subunit β cryptic class I ribonucleotide reductase	+2.47 ± 0.09
	SOS Network	
sulA	inhibits FtsZ ring formation	+1.48 ± 0.04
dinB	DNA polymerase IV	+0.85 ± 0.23
recA	recombinatorial repair	+0.97 ± 0.02
recN	recombinatorial repair	+0.71 ± 0.10
umuC	DNA polymerase V	+1.58 ± 0.28
umuD	DNA polymerase V	+1.49 ± 0.07
ruvA	Holliday junction recognition	+1.19 ± 0.31
ruvB	branch migration of Holliday structures	+1.58 ± 0.64
uvrB	excision nuclease subunit B	+1.52 ± 0.15
	Cell Division	
ftsZ	initiates septum ring formation	−1.29 ± 0.20
zipA	septal ring structural protein	−1.53 ± 0.09
ftsQ	growth of cell wall at septum	−0.93 ± 0.28
rcsB	*ftsZ* regulator	−0.71 ± 0.05
	DNA Replication Restart	
priA	primosome factor Y	+1.20 ± 0.24
priB	primosome protein	+1.04 ± 0.13
dnaB	helicase	+0.41 ± 0.14
dnaC	helicase loading	+0.95 ± 0.14
dnaN	sliding clamp subunit	+1.52 ± 0.12
	Iron Uptake	
fecA	receptor, citrate-dependent ferric iron transport	+2.03 ± 0.10
fecB	periplasmic protein, ferric iron transport	+1.80 ± 0.14
fecC	ferric iron transport	+1.77 ± 0.19
fecD	membrane protein, ferric iron transport	+1.31 ± 0.26
fecE	ferric iron transport	+1.58 ± 0.42
fecI	ferric iron transport	+2.16 ± 0.10
fecR	regulator of ferric iron transport	+1.12 ± 0.16
feoA	ferrous iron uptake system	+0.65 ± 0.20
feoB	membrane protein, ferrous iron uptake system	+0.76 ± 0.26
fepA	outer-membrane protein, ferribactin transport	+1.85 ± 0.08
fepB	periplasmic protein, ferrienterobactin transport	+1.19 ± 0.09

Table 1. *Continued*

Gene	Gene Product/Function	Z Score ± SE (+HU vs. −HU)
	Iron Uptake	
fepC	inner-membrane protein, ferrienterobactin transport	+1.51 ± 0.52
fepD	ferrienterobactin permease	+1.23 ± 0.24
fepG	ferrienterobactin permease	+1.40 ± 0.51
fhuA	ferrichrome OMP	+1.59 ± 0.22
fhuB	hydroxamate-dependent ferric uptake	+2.07 ± 0.57
fhuC	hydroxamate-dependent ferric uptake	+1.59 ± 0.26
fhuD	hydroxamate-dependent ferric uptake	+1.34 ± 0.28
fhuE	ferric-rhodotorulic acid outer-membrane receptor	+0.86 ± 0.25
fhuF	ferric hydroxamate transport	+2.38 ± 0.16
tonB	iron uptake	+1.88 ± 0.09
exbB	iron uptake	+2.43 ± 0.09
exbD	iron uptake	+2.11 ± 0.05
	Toxin-Antitoxin Pairs	
mazE	suppressor of MazF activity	−0.37 ± 0.02
mazF	toxic protein, growth inhibitor	+0.10 ± 0.35
relB	suppressor of RelE activity	−0.21 ± 0.08
relE	toxic protein, growth inhibitor	−0.04 ± 0.08

[1] SE, standard error.

fluorescence microscopy (Ma et al., 1996). Induction of FtsZ-GFP by IPTG was comparable in HU-treated and nontreated cultures (Figure S1H). Under nonstress conditions, we observed septal ring formation in MC4100 cells at midcell (Figure 1D). However, when *ftsZ*-GFP was induced following HU treatment, the elongated cells did not show Z ring formation (Figure 1D). In fact, we did not observe Z rings in any HU-treated cells (data not shown). Together, these results strongly suggest that the decreased expression of *ftsZ* and other septum assembly genes is sufficient to perturb normal septum formation.

HU-Induced Iron Uptake Response Is Nonuniform and Associated with Cell Death

We also observed several functional classes of genes whose expression changes we could not easily explain as survival responses. Our microarray analysis indicated that many genes encoding the Fep, Fec, Fhu, and Feo iron uptake systems (Postle and Larsen, 2007) were significantly upregulated after 1 hr of HU treatment (Table 1). Iron is required for numerous biological purposes, including playing a catalytic role in class I RNR (Stubbe, 2003), so it seemed possible that increased iron uptake in response to HU represents an effort to replenish RNR. However, excessive amounts of iron can be deleterious to *E. coli*, catalyzing the production of highly destructive hydroxyl radicals (OH•) through Fenton chemistry (Jakubovics and Jenkinson, 2001). To test whether such a strong HU-induced iron uptake had an overall beneficial or detrimental effect on *E. coli*, we disrupted *tonB*, which is a component of the TonB/ExbB/ExbD inner-membrane protein complex. TonB is important for iron uptake because it couples the dedicated outer-membrane iron transporters FepA, FecA, and FhuE to the proton-motive force
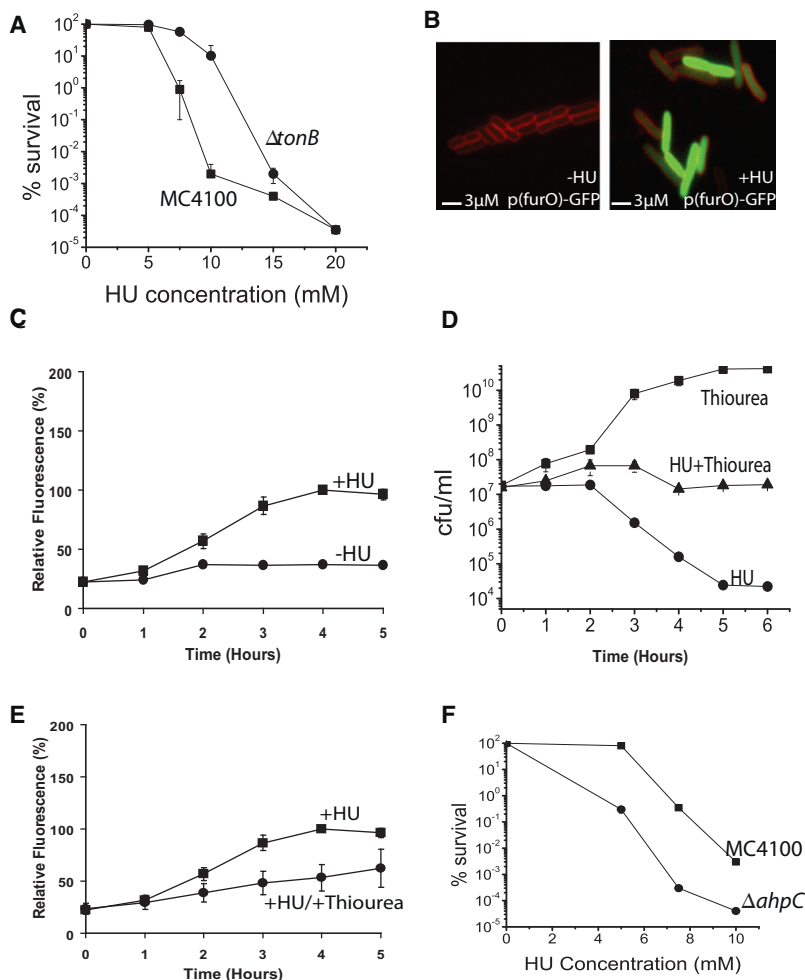
Figure 2. HU Treatment Induces Iron Uptake Response and Oxidative Stress

(A) MC4100 (■) and a ΔtonB mutant (●) were serially diluted and spotted on LB agar plates containing increasing concentrations of HU.

(B) Fur-regulated GFP-expressing cells were treated with 100 mM HU for 1 hr and then imaged. No GFP fluorescence was observed in the absence of HU (data not shown).

(C) Hydroxyl radical formation measured by HPF fluorescence in MC4100 treated with or without 100 mM HU. The relative fluorescence values were determined by taking the mean fluorescence value for each sample at each time point and normalizing that value to the maximum mean fluorescence value that the wild-type sample achieved over the time course. Each data point represents the average of three independent measurements of these relative fluorescence values, and the error bars represent SE of the independent measurements.

(D) Survival curve of MC4100 treated with 100 mM HU in the presence (■) or absence (●) of 100 mM thiourea. The growth of MC4100 in the presence of 100 mM thiourea is shown as a control (■).

(E) Hydroxyl radical formation measured by HPF fluorescence in MC4100 following treatment with 100 mM HU with or without 100 mM thiourea. Fluorescence for each condition is shown relative to the maximum fluorescence achieved by MC4100 + 100 mM HU.

(F) MC4100 (■) and ΔahpC (●) strains were spotted on LB agar plates containing increasing concentrations of HU.

(Wandersman and Delepelaire, 2004; Wiener, 2005). We found that disruption of *tonB* increased resistance of the strain to HU (Figure 2A), suggesting that the strong upregulation of iron uptake has an overall negative impact on cell survival under HU stress.

We asked whether the increased iron uptake occurred on the same timescale as HU-protective responses such as the SOS response. To explore the temporal relationship between iron uptake and HU treatment, we observed MC4100-carrying plasmid pL(*furO*)-GFP that expresses GFP under the control of the iron-responsive transcriptional regulator Fur. Fur controls expression of three major iron transport systems upregulated in our microarray: Fec, Fep, and Fhu. In contrast to induction of the SOS-regulated GFP response, we did not observe Fur-regulated GFP expression after 15 min of HU treatment and observed only minor induction at 30 min (Figure 1B, iii and iv). Under the same exposure conditions, we did observe a significant increase in Fur-regulated GFP expression after 1 hr of HU treatment, consistent with our microarray data (Figure 2B). Interestingly, our microscopy indicated that there were two subpopulations of GFP-expressing cells after 1 hr of HU treatment. Both subpopulations showed GFP fluorescence above the untreated

control, but one subpopulation was more fluorescent than the other.

We further explored the relationship between iron uptake and cell death by staining MC4100 cells carrying pL(*furO*)-GFP with propidium iodide. Propidium iodide is used as a marker for cell death, as it is only able to enter and stain bacteria that have damaged cell membranes. After 3 hr of HU treatment, we found that 20% of cells stained with propidium iodide and that 98% of propidium iodide-stained cells also showed increased levels of Fur-regulated GFP expression (n = 810 cells). In sum, these results indicated that, unlike the uniform SOS survival response, the induction of genes involved in iron uptake occurs later to two distinguishable levels and correlates with cell death.

Quenching of Hydroxyl Radicals Prevents HU-Induced Cell Death

We had speculated that increased iron uptake might be detrimental to the cell by increasing OH• formation (Imlay et al., 1988). To test this idea, we monitored the fluorescence of the dye, 3′-(ρ-hydroxyphenyl)-fluorescein (HPF), in cultures after HU treatment (Kohanski et al., 2007). HPF is oxidized with high specificity by OH• to a fluorescent product (Setsukinai et al., 2003). One hour after HU treatment, we observed OH• formation in MC4100 that steadily increased until reaching a maximum at 4 hr (Figure 2C). The first major increase in OH• formation coincides exactly with the first major decrease in cell viability after HU exposure (Figure 1A). This correlation suggests that
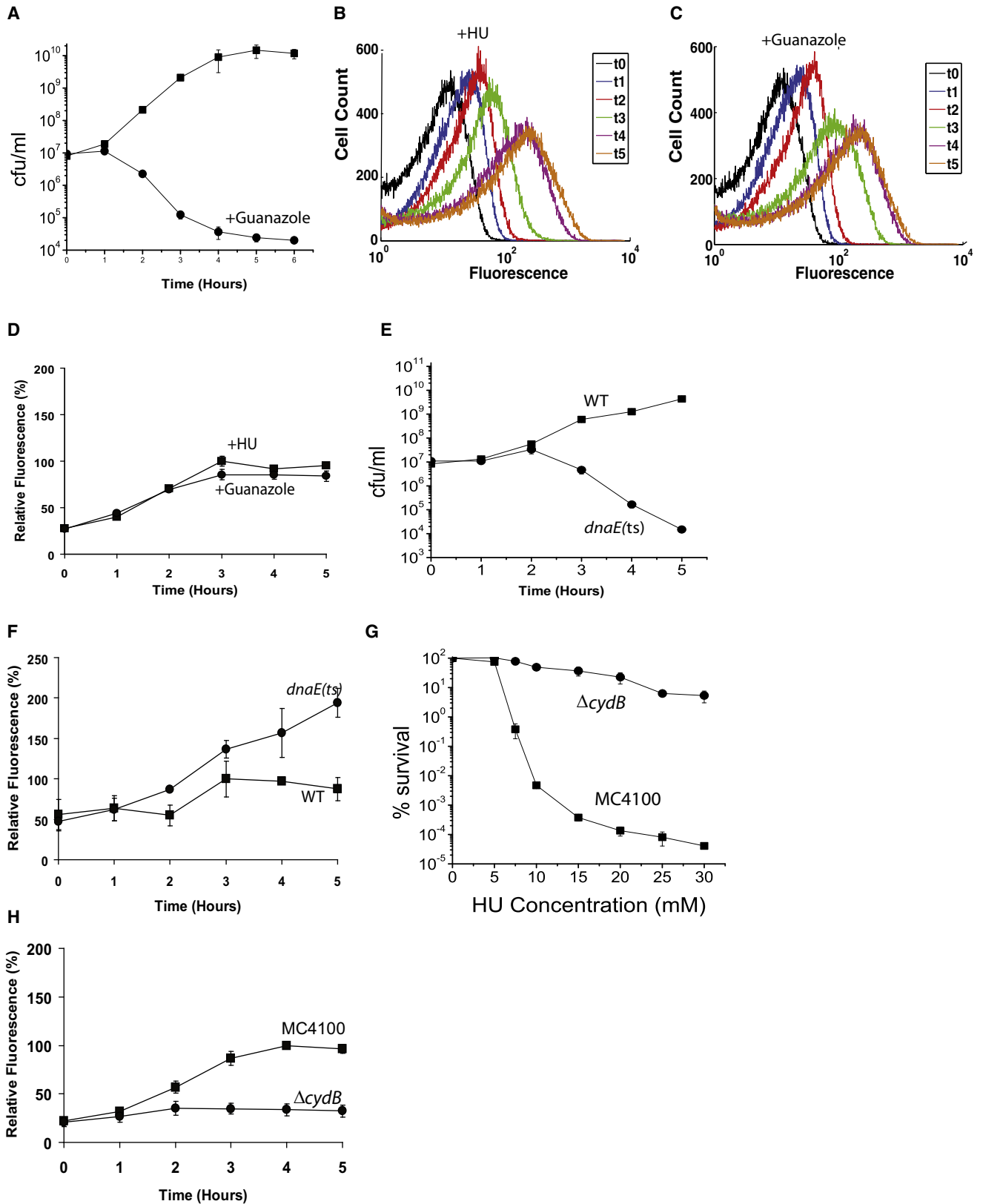
HU-induced cell death may be due, at least in part, to increased OH• levels.

To test whether the increased OH• production that we observe following HU treatment is causally related to cell death, we quenched OH• using the potent OH• scavenger thiourea (Novogrodsky et al., 1982; Repine et al., 1981; Touati et al., 1995). Though similar in structure to HU, thiourea is not a potent inhibitor of RNR because it lacks the key hydroxyl group that inactivates RNR and thus does not affect culture growth (Figure 2D) (Stubbe, 2003). Addition of thiourea to cultures essentially prevented HU-induced cell death (Figure 2D) and strongly decreased OH• formation (Figure 2E). In other words, thiourea changes HU from a bactericidal stress into a bacteriostatic stress. Thiourea did not interfere with the HU-dependent arrest of DNA synthesis (Figure S2B). Because thiourea has been shown to scavenge another radical, HOCl (Wasil et al., 1987), we cannot rule out the possibility that thiourea may be quenching additional unknown radicals that also contribute to HU-induced cell death. Nevertheless, the virtually complete abrogation of cell death brought about by thiourea treatment strongly suggests that OH• and possibly other radicals play a causal role in the chain of events that leads to cell death in response to prolonged HU treatment.

OH• formation via the Fenton reaction occurs when hydrogen peroxide (H_2O_2) interacts with ferrous iron. There are a number of enzymes that can remove harmful reactive oxygen species (ROS), and in *E. coli*, *ahpCF* encodes for one of the key H_2O_2-scavenging enzymes (Seaver and Imlay, 2001). We examined survival of an Δ*ahpC* strain and found that loss of *ahpC* increased sensitivity to HU through a range of HU concentrations (Figure 2F). This result strongly supports our inference that HU induces OH• formation via Fenton chemistry and that this ROS contributes to HU-mediated cell death.

Replication Fork Arrest Promotes OH• Production

Our results indicate that OH• play a causal role in HU-mediated cell death, yet blocking iron uptake by deleting *tonB* results in only a modest increase on survival in the presence of HU. Thus, though increased iron likely contributes to HU-mediated cell death by promoting OH• formation, our results suggest that there must be additional factors responsible for the high levels of OH• production after HU treatment.

Although RNR is widely thought to be the sole cellular target of HU (Fuchs and Karlstrom, 1973; Kren and Fuchs, 1987; Sjoberg et al., 1986; Sneeden and Loeb, 2004), it was still possible that the increased iron uptake and OH• production, which contribute to cell death, were off-target effects of HU treatment. To address these issues, we first treated MC4100 with guanazole and again monitored for increased iron uptake and hydroxyl radical formation. Guanazole is a highly specific inhibitor of RNR that is chemically distinct from HU (Foti et al., 2005; Jones et al., 2007; Moore and Hurlbert, 1985). Treatment of MC4100 with 100 mM guanazole resulted in ~0.1% survival after 6 hr, similar to HU treatment (Figure 3A). We monitored iron uptake using plasmid pL(*furO*)-GFP. Treatment of MC4100 carrying pL(*furO*)-GFP with either HU (Figure 3B) or guanazole (Figure 3C) resulted in a substantial increase in Fur-regulated GFP fluorescence, as measured by flow cytometry. Furthermore, treatment of MC4100 with guanazole also strongly induced OH• production (Figure 3D). These results support the hypothesis that both increased iron uptake and OH• production are due to inhibition of RNR activity rather than an off-target effect of HU.

To determine whether increased iron uptake and OH• were due strictly to the inhibition of RNR or to the downstream effects of replication fork arrest, we tested a temperature-sensitive *dnaE* mutant (Strauss et al., 2005) for iron uptake and OH• production at the permissive and nonpermissive temperatures. *dnaE* codes for the α-catalytic subunit of DNA polymerase III holoenzyme and is essential for DNA synthesis (Gefter et al., 1971; Wickner and Kornberg, 1974), and incubation at the nonpermissive temperature leads to replication fork arrest in the *dnaE*(ts) mutant. At the permissive temperature, the *dnaE*(ts) strain was identical to the parental strain with respect to growth, expression of iron uptake, and OH• formation (data not shown). After 5 hr at the nonpermissive temperature of 40°C, the *dnaE*(ts) strain viability had decreased to 0.1% (Figure 3E). Of interest, at the nonpermissive temperature, the *dnaE*(ts) strain did not exhibit a change in iron uptake response (Figures S2B and S2C) but did show a significant increase in OH• formation (Figure 3F) compared to the wild-type control strain. In fact, the first major increase in OH• production was observed at the same time as the first major decrease in *dnaE*(ts) mutant cell survival. These observations support our conclusion that, in addition to the increase in iron uptake caused by HU treatment, there must be additional cellular responses resulting from the blocked replication fork that play a major role in OH• production and subsequent cell death.

The major source of reactive oxygen species in the cell is from the inappropriate reduction of oxygen during electron transport through the respiratory chain (Imlay and Fridovich, 1991). It

Figure 3. Effects of Replication Fork Arrest

(A) Survival curve of MC4100 treated with (●) or without (■) 100 mM guanazole.

(B and C) MC4100 pL(*furO*)-GFP treated with 100 mM HU or 100 mM guanazole and sorted by flow cytometry as previously described (Dwyer et al., 2007).

(D) Comparison of hydroxyl radical formation measured by HPF fluorescence in MC4100 treated with HU (■) or guanazole (●) normalized to MIC. Fluorescence for each strain is shown relative to the maximum fluorescence achieved by MC4100 + 100 mM HU.

(E) Survival curve of the *dnaE*(ts) mutant (●) and parental strain (■) grown at the nonpermissive temperature.

(F) Hydroxyl radical formation measured by HPF fluorescence in the *dnaE*(ts) (●) and parental strain (■) grown at the nonpermissive temperature. Fluorescence for each strain is shown relative to the maximum fluorescence achieved by the wild-type strain.

(G) MC4100 (■) and Δ*cydB* (●) strains were spotted on LB agar plates containing increasing concentrations of HU.

(H) Hydroxyl radical formation measured by HPF fluorescence in MC4100 (■) and the Δ*cydB* mutant (●) during HU treatment. Fluorescence for each strain is shown relative to the maximum fluorescence achieved by MC4100 + 100 mM HU.

Each data point represents the average of at least three independent experiments, and the error bars represent the standard error of the independent measurements.

was recently shown that lethality of a temperature-sensitive DNA polymerase III mutant could be overcome (Strauss et al., 2005) by disrupting one the major respiratory cytochrome oxidases, cytochrome oxidase bd (Poole and Cook, 2000; Strauss et al., 2005). We hypothesized that replication fork arrest was ultimately disrupting electron transport chain activity, which was leading to increased ROS production. Agreeing with this, we found that deleting *cydB*, which encodes subunit b of one of the major respiratory terminal cytochrome oxidases, prevented HU-induced cell death (Figure 3G). Furthermore, deletion of *cydB* nearly completely prevented HU-induced OH• formation (Figure 3H).

mazEF and *relBE* Act Synergistically to Promote Cell Death and OH• Production and Are Additive in Their Effects with Increased Iron Uptake

Our observations that the *dnaE*(ts) mutant produced OH• at the nonpermissive temperature and that the Δ*cydB* mutant exhibited increased survival following HU treatment point toward replication fork arrest as a key element underlying ROS formation during HU stress. It was also recently shown that the action of MazF can mediate cell death in response to certain antibiotics by producing reactive oxygen species (Kolodkin-Gal et al., 2008). Of interest, we had previously shown that disruption of either toxin-antitoxin pairs, *mazEF* or *relBE*, in the *E. coli* HM21 and P90C strain backgrounds increased HU resistance (Godoy et al., 2006). These observations led us to ask whether the *mazEF* and *relBE* toxin/antitoxin modules contributed to the death of HU-treated strain MC4100 via an OH•-mediated mechanism and whether this is connected to HU-mediated replication fork inhibition. When challenged with HU, we found that, in strain MC4100, deletion of *mazEF* led to increased resistance to HU (Figure 4A). The MC4100 Δ*relBE* strain, however, was indistinguishable from the parental strain for HU survival (Figure 4B). Strikingly, we found that deletions of both *mazEF* and *relBE* act synergistically to promote HU resistance to levels far above that observed in a Δ*mazEF* strain alone (Figure 4C) and similar to that observed with the Δ*cydB* strain. Deletion of *relBE* did not have a detectable effect on OH• formation, whereas deletion of *mazEF* caused a small decrease in OH• formation (Figures S2D and S2E). The Δ*mazEF* Δ*relBE* strain exhibited a stronger reduction in OH• levels (Figure S2F), consistent with the observed increase in survival (Figure 4C). We also note that our microarray results showed that HU induced only small increases in expression of *mazF* relative to *mazE* and of *relE* relative to *relB* (Table 1), suggesting that HU treatment appears to be affecting toxin activation mainly at a posttranscriptional level.

We have shown above that increased iron uptake has overall negative effects on HU survival. To determine the relationship between increased iron uptake and toxin-induced cell death, we constructed a Δ*mazEF* Δ*relBE* Δ*tonB* strain and tested its sensitivity to HU. We found that our Δ*mazEF* Δ*relBE* Δ*tonB* was more resistant to HU than was our Δ*mazEF* Δ*relBE* strain (Figure 4D). This suggests that increased iron uptake enhances toxin-mediated cell death, which likely occurs via an OH•-dependent mechanism. Consistent with these data, we found that deleting *tonB* in combination with Δ*mazEF* Δ*relBE* results in a significant decrease in the levels of OH• following HU treatment (Figure 4E).

Toxin Activity Leads to Improperly Translated Proteins and Membrane Stress

We next considered how toxin activity could lead to radical-mediated cell death. A number of chromosomally encoded toxins have functions that directly affect protein synthesis. HipA was recently shown to phosphorylate the translation-related protein EF-Tu (Schumacher et al., 2009), and the toxins MazF and RelE are ribonucleases that cleave mRNA (Christensen and Gerdes, 2003; Zhang et al., 2005), thereby disrupting protein translation. Improper protein synthesis can lead to problems with protein folding, and this has been associated with protein carbonylation (a marker of oxidative stress) (Dukan et al., 2000) and ROS formation following treatment with aminoglycosides (Kohanski et al., 2008). Recent work has also shown that MazF overexpression can lead to protein carbonylation (Kolodkin-Gal et al., 2008). We hypothesized that HU stimulates MazF and RelE activity, which cleave mRNA, leading to truncated proteins, protein misfolding, and, ultimately, oxidative stress and cell death.

To test this idea, we investigated protein translation following HU treatment to determine whether replication fork inhibition affects protein synthesis and whether such an effect is toxin dependent. Disruption of protein translation can lead to stalled ribosomes that can be rescued by tmRNA (Moore and Sauer, 2007). tmRNA frees stalled ribosomes by releasing both mRNA and the incompletely translated protein. We used the tmRNA system developed by Moore et al., which adds a 6× His peptide tag to the end tmRNA-released proteins, to monitor the effect of toxin activity during HU treatment (Moore and Sauer, 2005). We found that HU treatment induced a significant increase in tmRNA His-tagged proteins (Figure 5A). This increase in tmRNA His-tagged proteins was alleviated by deleting both toxins MazF and RelE. This suggests that toxin activity during HU treatment likely leads to the improper translation of proteins.

Improperly translated proteins can also lead to membrane stress (Alba and Gross, 2004). To test whether the HU treatment leads to membrane stress, we first used an *rpoHP3-lacZ* reporter to measure RpoE activity following HU treatment. RpoE is a σ factor whose activity is induced by membrane stress (Alba and Gross, 2004). After only 1 hr of HU treatment, we observed a 2-fold increase in RpoE activity (Figure 5B). This increase in RpoE activity was prevented by deletion of both toxins MazF and RelE, confirming that toxins stimulate envelope stress, likely through a mechanism involving improperly translation proteins. We were unable to assess RpoE activity at later time points because the strain lacking both toxin-antitoxin pairs rapidly approached stationary phase, which induces RpoE activity (Kabir et al., 2005).

To confirm that membrane stress affects HU-mediated survival, we looked at the responses of Δ*cpxA* and Δ*degP* mutant strains to HU treatment. Disruption of membrane proteins also leads to the activation of the CpxAR two-component signaling system (CpxA is the sensor protein, and CpxR is the cognate transcription factor), which monitors the fidelity of proteins trafficked across the inner membrane and works in conjunction with σ[E] to activate elements of the envelope stress response system such as the periplasmic protease, *degP* (MacRitchie et al., 2008; Ruiz and Silhavy, 2005). Recent evidence suggests that mistranslated proteins can induce OH• through Cpx-mediated
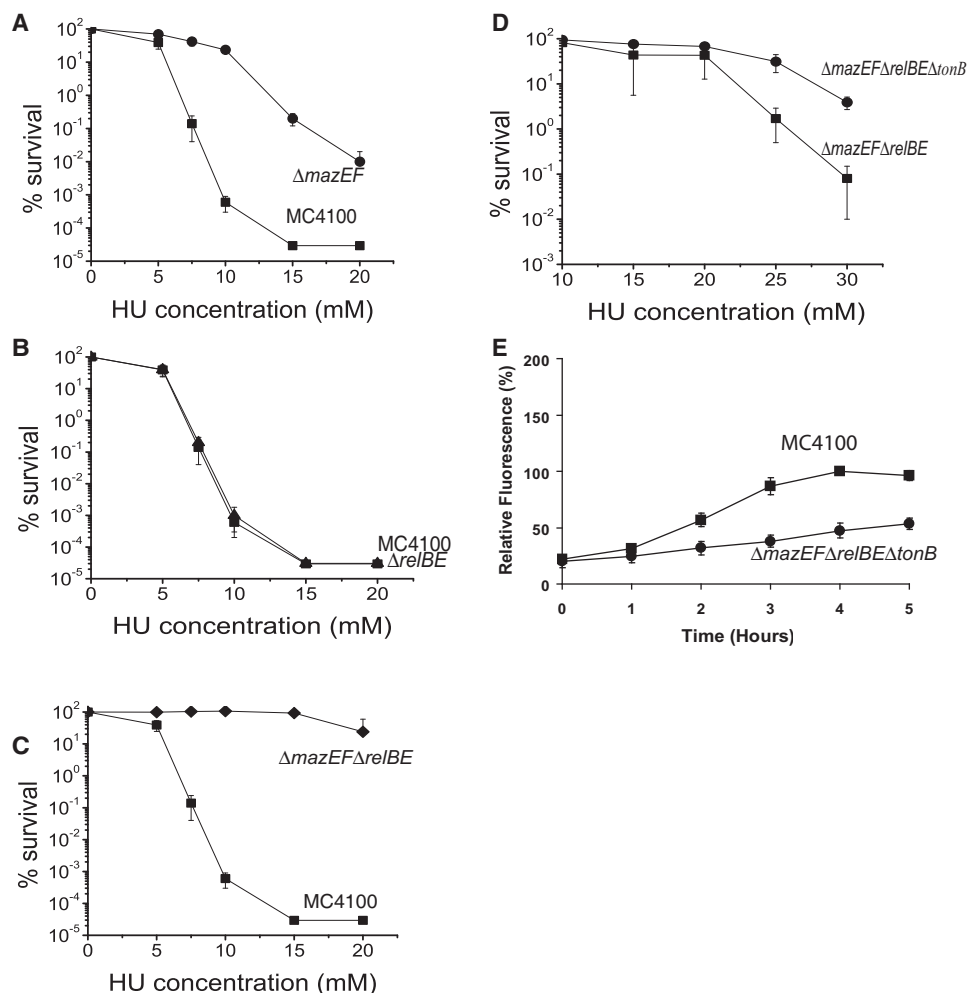
Figure 4. HU Stress Assays

(A–D) (A) MC4100 (■) and Δ*mazEF* (●), (B) MC4100 (■) and Δ*relBE* (●), (C) MC4100 (■) and Δ*relBE* Δ*mazEF* (◆), and (D) Δ*relBE* Δ*mazEF* (■) and Δ*relBE* Δ*mazEF* Δ*tonB* (●). Strains were spotted on LB agar plates containing increasing concentrations of HU.

(E) Hydroxyl radical formation measured by HPF fluorescence in MC4100 (■) and the Δ*relBE* Δ*mazEF* Δ*tonB* mutant (●) in the presence of 100 mM HU using flow cytometry. Fluorescence for each strain is shown relative to the maximum fluorescence achieved by MC4100 + 100 mM HU.

Each data point represents the average of at least three independent experiments, and the error bars represent the standard error of the independent measurements.

perturbation of envelope stress and metabolism and that deletion of the *cpxA* or *degP* significantly decreased OH• production (Kohanski et al., 2008). In agreement with this, we found that deletion of *cpxA* resulted in a striking rescue from HU-induced cell death (Figure 5C), comparable to that achieved by deleting *cydB* or *mazEF*, *relBE*, and *tonB*. Deletion of *cpxA* also substantially reduced HU-induced OH• production (Figure 5D). Furthermore, we also observed that deletion of *degP* also conferred significant resistance to HU-induced cell death (Figure 5C).

HU Treatment Leads to Membrane Depolarization and Toxin-Mediated Release of Superoxide

If HU-induced membrane stress leads to OH• formation by disrupting the normal electron flow through the electron transport chain, then we hypothesized that HU treatment should also lead to changes in membrane potential. We treated cells with the bisoxonol dye DiBAC, which diffuses across depolarized yet intact cell membranes (Jepras et al., 1997). We examined cells 3 hr after HU treatment, as cell death appears to have begun by this time (Figure 1A), and observed a significant number of DIBAC-stained cells (Figure 5F). Furthermore, we found that only cells strongly expressing Fur-regulated GFP stained with DIBAC (Figure 5G). This agrees with our observation above that, overall, increased expression of iron uptake genes is associated with HU-induced cell dysfunction.

The most common ROS released from the respiratory chain is superoxide (Imlay and Fridovich, 1991). Our results demonstrating a connection between toxin activity and membrane stress, together with our earlier results showing that Δ*cydB* is
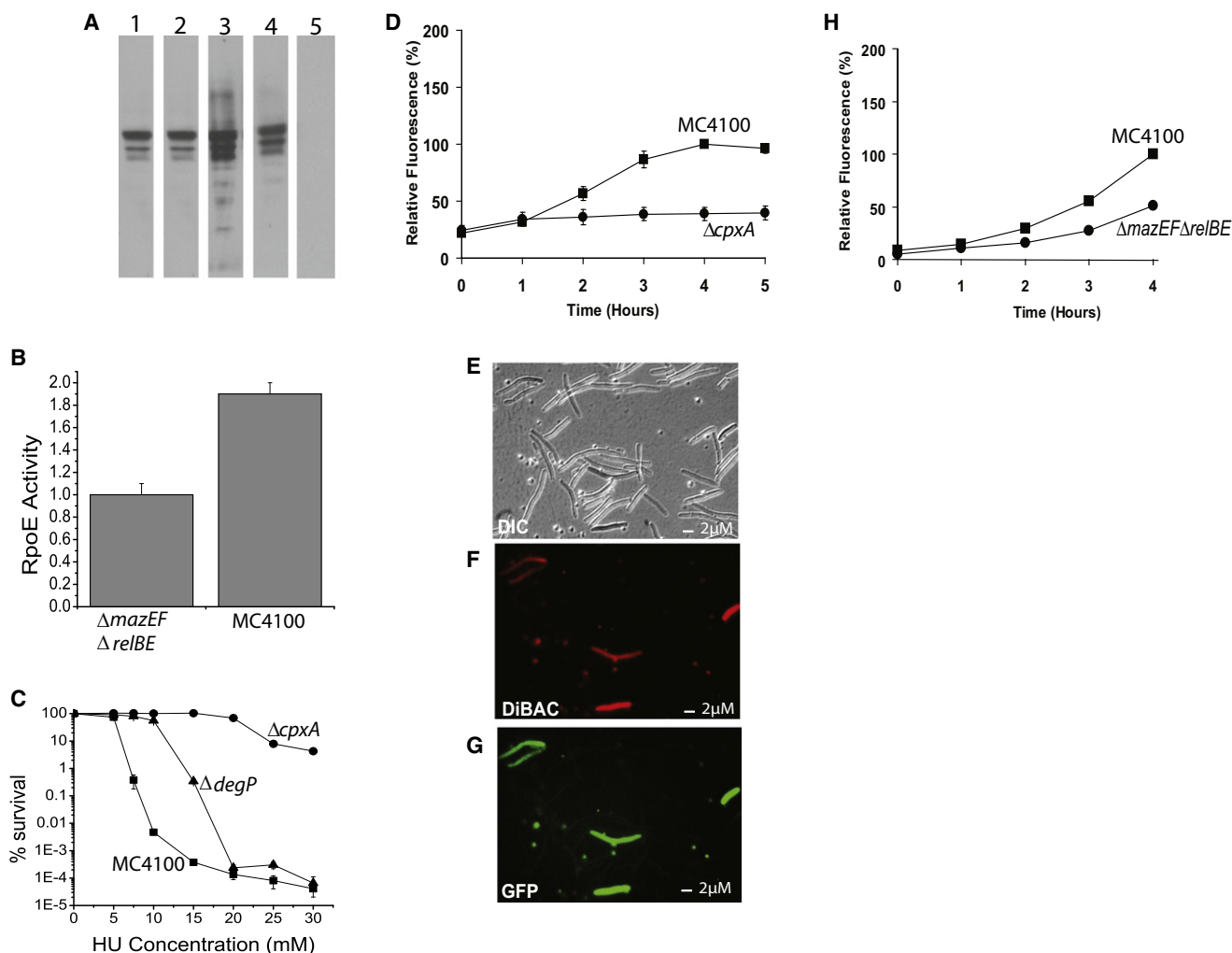
Figure 5. HU Treatment Induces Membrane Stress

(A) MC4100 and the Δ*relBE* Δ*mazEF* mutant carrying the tmRNA-6× His allele were treated with or without 100 mM HU for 3 hr. Equal amounts of total protein lysate were separated by SDS-PAGE and probed with a monoclonal anti-His antbody. Lane 1, MC4100 (–) HU; lane 2, Δ*relBE* Δ*mazEF* (–) HU; lane 3, MC4100 (+) HU; lane 4, Δ*relBE* Δ*mazEF* (+) HU; lane 5, MC4100 without tmRNA-6× His (+) HU.

(B) MC4100 and the Δ*relBE* Δ*mazEF* carrying reporter *rpoH*P3-*lacZ* treated with or without HU for 1 hr. The plot shows the ratio of *lacZ* activity with or without HU for each strain.

(C) MC4100 (■), Δ*cpxR* (●), and Δ*degP* (■) strains were spotted on LB agar plates containing increasing concentrations of HU.

(D) Hydroxyl radical formation measured by HPF fluorescence in MC4100 (■) and the Δ*cpxA* mutant (●) in the presence of 100 mM HU using flow cytometry.

(E–G) Fur-GFP-containing cells were treated with 100 mM HU for 3 hr. The culture was then stained with DiBAC. (E) Nomarsky image of cells. (F) Image showing DIBAC staining. (G) Image showing Fur-regulated GFP expression.

(H) MC4100 pL(*soxR*)-GFP (■) and Δ*relBE* Δ*mazEF* pL(*soxR*)-GFP (●) treated with 100 mM HU and sorted by flow cytometry.

Each data point represents the average of at least three independent experiments, and the error bars represent the standard error of the independent measurements.

substantially less sensitive to HU treatment, suggest that HU-induced changes in membrane composition and function may lead to superoxide formation. Superoxide is converted to hydrogen peroxide (H_2O_2) that can react with ferrous iron to produce OH• (Jakubovics and Jenkinson, 2001). It is thus possible that toxin-mediated superoxide formation can contribute to an increase in Fenton chemistry, which would explain the significant decrease in cell death in the Δ*mazEF* Δ*relBE*

Δ*tonB* strain. To monitor superoxide production, we used plasmid pL(*soxS*)-GPF, which expresses GFP under the control of the superoxide-sensing regulator SoxS (Dwyer et al., 2007). We observed an increase in SoxS-regulated GFP expression following HU treatment. SoxS-regulated GFP expression was significantly decreased in the Δ*mazEF* Δ*relBE* mutant (Figure 5H), which demonstrates that HU-mediated toxin activity contributes to cell death via superoxide formation.
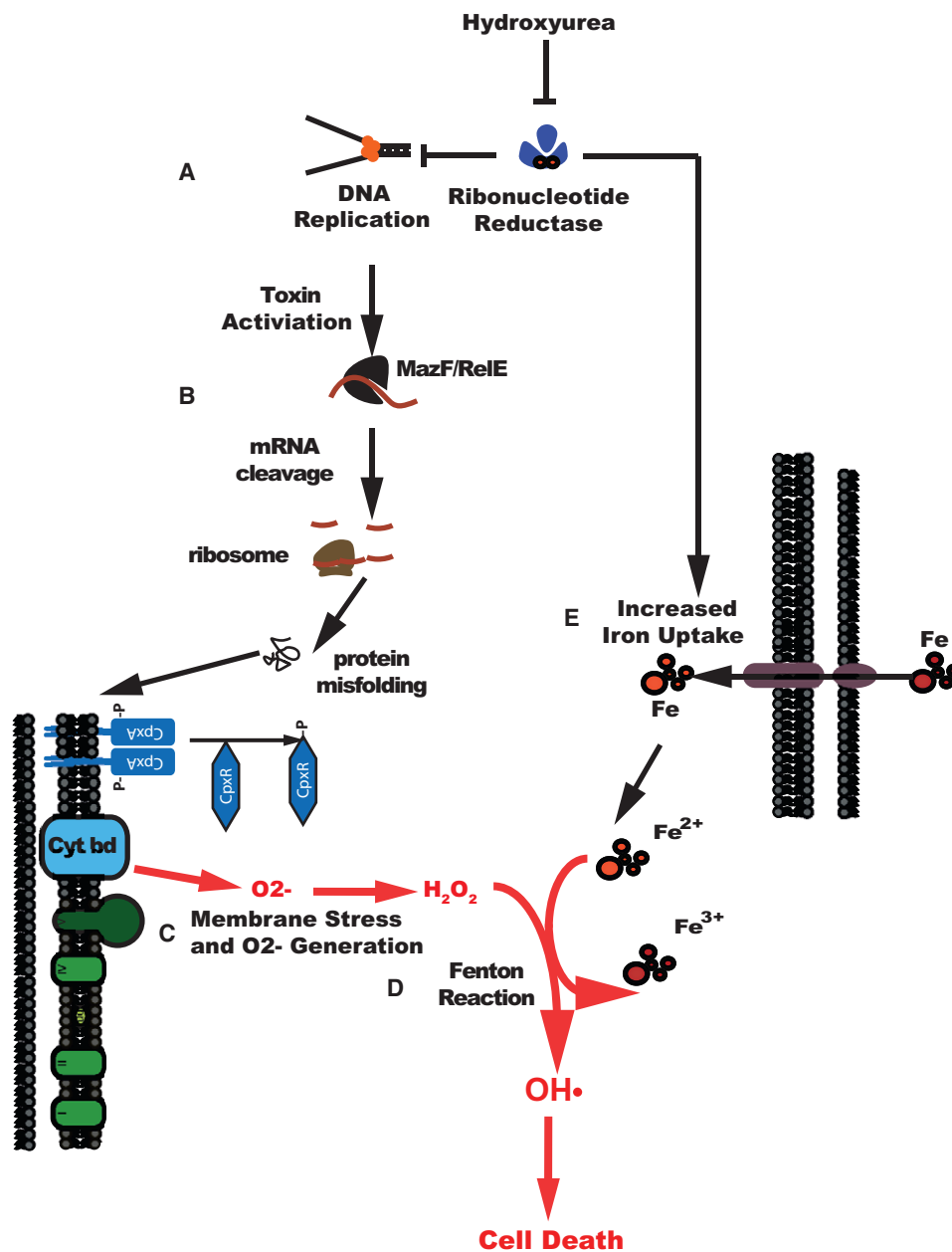
Figure 6. Schematic Representation of Cellular Response to HU Treatment

(A) In *E. coli*, HU rapidly inhibits RNR, arresting replication fork progression.

(B) Subsequent activation of toxins MazF and RelE leads to improperly translated proteins, membrane stress, and membrane stress responses.

(C and D) (C) These effects disrupt respiratory chain activity, causing an increase in superoxide production, eventually leading to increased OH• production and (D) cell death.

(E) Misregulation of the HU-induced iron uptake response further fuels this processes by increasing the amount of free iron available for Fenton chemistry.

DISCUSSION

Our work describes the previously unknown chain of events by which HU-induced DNA replication arrest leads to cell death. On the basis of our findings, we propose the following mechanism whereby HU treatment results in cell death (Figure 6). HU inhibits RNR, leading to dNTP depletion and an arrest of normal DNA replication (Figure 6A). dNTP depletion results in the activation of toxins MazF and RelE. The activity of these toxins produces improperly translated proteins, leading to membrane stress and activation of membrane stress responses (Figure 6B). These effects alter the properties of one of the cell's two terminal cytochrome oxidases in the electron transport chain, causing an increase in the production of superoxide, which is then

converted to hydrogen peroxide (Figure 6C). The hydrogen peroxide reacts with free ferrous iron, resulting in the formation of OH•, which contribute to cell death (Figure 6D). HU treatment also induces a strong iron uptake response (Figure 6E), which may be part of an initial survival response to increased demand for synthesis of the iron-utilizing class I RNR. However, due to replication fork arrest, toxin activity, and membrane stress, HU-induced iron uptake becomes misregulated and exacerbates OH• production (Figure 6E).

Our work also shows that HU initially induces cell survival responses beyond the classic SOS response. Specifically, we show that HU induces genes required for primosome formation and downregulates genes required for cell division. Induction of primosome genes could help restart collapsed replication forks that have resulted from HU treatment. Downregulation of cell division genes would retain all copies of the chromosome in one compartment, thus leaving open the possibility of recombinational repair.

It is striking that HU-induced death, which takes several hours and is preceded by specific cellular changes and is associated with cell lysis, can be substantially prevented by adding thiourea or by inactivating *cydB*, *cpxA*, or the combination of *mazEF*, *relBE*, and *tonB*. These systems appear to converge on radical formation as a contributing element in HU-mediated cell death, and these observations suggest that there is one predominant mode of death for HU-treated cells, which is in contrast to cells treated with various bactericidal antibiotics for which there are additional modes of death besides that mediated by OH• radicals (Kohanski et al., 2007).

Of interest, Kohanski et al. (2007) showed that treatment of *E. coli* with the DNA gyrase inhibitor norfloxacin also induces radical production and cell death, both of which can be partially alleviated by thiourea. However, thiourea rescue of norfloxacin-induced cell death is not as complete as it is for HU. Thus, though both HU and norfloxacin inhibit DNA replication and induce lethal radical production, radicals appear to play a more significant role in HU-induced cell death. We believe that this difference is due to the exact mode of replication arrest that these two compounds elicit and how the cell interprets these modes of replication arrest. A clue that this may be the case comes from microarray studies that show that norfloxacin does not induce iron uptake but does cause internal iron release by destabilizing iron-sulfur clusters (Kohanski et al., 2007). Furthermore, norfloxacin-mediated radical production is not dependent on toxins, whereas HU radical production is.

Our observations establish a direct link between HU-mediated killing and the respiratory chain (Figure 6C) and suggest that, under the stressed condition resulting from prolonged exposure to HU, the *cydAB*-encoded heterodimeric cytochrome *bd* quinol oxidase plays a contributing role in cell death by generating superoxide. The involvement of this particular cytochrome in HU-mediated cell death is intriguing. Typically, cytoplasmic superoxide is not generated by the action of cytochrome oxidases (Imlay, 2003), and both cytochrome *bd* and cytochrome *bo₃* have molecular features that prevent the release of incompletely reduced oxygen as superoxide (Tsubaki et al., 2000). Nevertheless, our results suggest that, under conditions of HU stress, cytochrome *bd* oxidase switches from a protective role

to a diametrically opposite role of promoting cell death by producing superoxide. From this perspective, it is intriguing that the *d* heme, which binds the O_2, is only found in this enzyme (Dueweke and Gennis, 1991).

Another unique feature of cytochrome *bd* oxidase is that its most prominent stable form is the one-electron reduced oxy state (Fe^{2+}-O_2) in which oxygen is at the level of superoxide (Belevich et al., 2005; Lorence and Gennis, 1989; Yang et al., 2008). Thus, it is possible that some modification of the cytochrome *bd* oxidase under conditions of prolonged HU stress could alter its function so that it becomes a producer of superoxide. Such a modification of function could result from a proteolytic cleavage in the stressed cells, perhaps in its protease-sensitive periplasmic loops (Dueweke and Gennis, 1991), in a manner reminiscent of the cleavage of RseA by DegS in response to envelope stress, or in a membrane-spanning domain by RseP (Ades, 2008). Other possibilities include C-terminal truncation by translation of an incomplete message, posttranslation modification, or modulation of the native enzyme by other components present in the stressed cell envelopes. Such alterations could, for example, potentially interfere with the efficiency of electron transfer from ubiquinol to the O_2-binding *d* heme or change the status of the putative O_2 channel that has been postulated to flicker between open and closed conformations under normal conditions (Belevich et al., 2007). The clustering of cytochrome *bd* oxidase in mobile patches in the membrane (Lenn et al., 2008) might have the effect of speeding up killing by concentrating hydroxyl radical production in particular regions of the cell.

Toxin/antitoxin modules are found both on plasmids and on bacterial chromosomes. It is widely accepted that the toxin/antitoxin pairs located on plasmids serve as "addiction" modules by killing bacteria that have lost the plasmid (Couturier et al., 1998; Engelberg-Kulka et al., 2006; Gerdes et al., 2005; Hayes, 2003; Jensen and Gerdes, 1995). There is evidence suggesting that toxin/antitoxin modules serve as growth modulators that help bacterial cells to manage a variety of physiological stresses (Buts et al., 2005; Gerdes et al., 2005). The proposal that chromosomally encoded TA pairs may mediate cell death in response to certain stresses has proven to be controversial (Engelberg-Kulka et al., 2006; Gerdes et al., 2005; Kolodkin-Gal and Engelberg-Kulka, 2006; Magnuson, 2007; Saavedra De Bast et al., 2008; Tsilibaris et al., 2007).

A recent study has shown that *mazEF*-mediated cell death appears to occur via ROS-dependent and independent mechanisms, which depends on the production of a density-dependent pentapeptide extracellular death factor (EDF) (Kolodkin-Gal et al., 2008). Furthermore, it has been suggested that the commonly used *E. coli* strain MG1655 is largely resistant to *mazEF*-mediated killing because it fails to produce the EDF and responds very poorly to it (Kolodkin-Gal and Engelberg-Kulka, 2008). Although the killing that results from HU exposure is mediated, in part, by *mazEF*, it differs from the *mazEF*-mediated killing discussed above in two important respects. First, we found that HU-induced cell death is independent of culture density (Figure S3A), indicating that activation of HU-induced cell death responses may not require the pentapeptide extracellular death factor described by Kolodkin-Gal and colleagues

(Kolodkin-Gal et al., 2007). Second, we found that HU induces cell death and lysis in strains MC4100 and MG1655 with similar kinetics (Figure S3B). Our results suggest that, although HU induces cell death responses that are at least partially dependent on toxin activation, these responses are complex (Figure 6) and quite different from those previously studied (Saavedra De Bast et al., 2008; Tsilibaris et al., 2007).

The mechanism by which HU-mediated dNTP depletion activates the MazF and RelE toxins and causes envelope stress is not yet clear. We hypothesize that HU-dependent depletion of dNTPs and subsequent replication fork arrest lead to gaps in the DNA that interrupt transcription and subsequent translation of several genes, including toxin/antitoxin pairs. Because antitoxins are more labile than their toxin counterparts are (Buts et al., 2005; Engelberg-Kulka et al., 2006), inhibition of transcription and translation could lead to rapid loss of antitoxin and activation of toxin. Possible support for this hypothesis comes from our previous observation that certain *umuC* mutations, such as *umuC122*::Tn5, permit DNA Pol IV (DinB) and DNA Pol V (UmuD′$_2$C) to carry out limited mutagenic DNA synthesis that makes cells resistant to killing by HU (Godoy et al., 2006). The K_ms of DNA Pol IV and Pol V for dNTPs are strikingly lower than those for the replicative DNA polymerase, explaining why they can act in dNTP-depleted cells (Godoy et al., 2006). This limited DNA synthesis presumably stabilizes the replication fork by filling in gaps that would otherwise accumulate under low-dNTP conditions.

In this work, we used a systems-level approach to examine the transcriptional response of *E. coli* following HU treatment and, in doing so, expanded our understanding of the events following HU-mediated RNR inhibition and replication fork arrest. We have explored the protective responses induced by HU treatment as well as responses that are important for cell death, and we implicate toxin-antitoxins, envelope stress, cytochromes, and iron misregulation as key players in an HU-mediated, free radical-based cell death pathway (Figure 6). Moving forward, it will be interesting to determine whether the cell death mechanism that we propose in this work extends past HU inhibition to encompass replication inhibition in general.

EXPERIMENTAL PROCEDURES

Strains, Plasmids, and Growth Conditions

Strains and plasmids are shown in Table S2. All strains were grown in Luria-Berani (LB) or M63 minimal medium (+ 0.2% glucose) at 37°C. For *ftsZ*-GFP assays, LB was supplemented with 0.2% glucose and 1.0 μM to 2.5 μM IPTG. Where indicated, antibiotics were used at the following concentrations: ampicillin (100 μg/ml except for BWD05 that used 25 μg/ml), kanamycin (30 μg/ml), and spectinomycin (100 μg/ml). Allele transfers were done by P1 transduction.

RNA Isolation and Microarray Analysis

MC4100 was grown to exponential phase. Three independent cultures were diluted and grown with or without 100 mM HU (Sigma) for 1 hr, after which RNA was isolated using the QIAGEN RNeasy extraction kit and samples were treated with DNase treated using DNA-free (Ambion). cDNA preparation and microarray analysis were performed as described (Dwyer et al., 2007). Results are reported as the average ± standard error (SE).

The resulting microarray *.CEL files were combined with *.CEL files from arrays that comprise the M3D compendium (Faith et al., 2007) (http://m3d.

bu.edu; E_coli_v3_Build_3) and were RMA normalized (Bolstad et al., 2003) with RMAexpress for a total of 530 RMA-normalized *E. coli* expression arrays. Each gene's SD of expression, σ, was calculated across the entire compendium and used to construct the z scale difference between that gene's normalized expression following hydroxyurea treatment versus the untreated control:

$$\Delta z_{exp} = \frac{X_{exp} - X_{ctl}}{\sigma}$$

This allowed us to measure each gene's change in expression for a given experiment in units of SD, a form of the z test. We used a two-tier z score cutoff platform to identify statistical significance gene expression changes. Genes with a z score of $> +2$ or < -2 were scored as highly significant, and genes with z scores between +1 and +2 or between −1 and −2 were scored as significant. As described in the manuscript, we tested candidate genes that showed statistically significant gene expression changes from our microarray analysis for biological significance in response to HU treatment.

Hydroxyurea, Guanazole, and Temperature Sensitivity Assays

Liquid culture assays were performed as described (Godoy et al., 2006). Exponentially growing cultures were diluted to OD$_{600}$ 0.01 or 0.0001 prior to treatment. Where indicated, HU, guanazole, and thiourea were added to 100 mM for liquid culture assays. For temperature sensitivity assays, exponentially growing cultures were diluted to OD$_{600}$ 0.01 and then shifted to the nonpermissive temperate. For chronic assays, strains were serially diluted and plated on LB agar containing increasing amounts of HU. Cfu were counted after 24 hr growth at 37°C. We required 100 mM HU to observe significant cell death in liquid culture and between 5 mM and 30 mM to observe significant cell death in plating assays. This is due the decreased stability of HU of liquid culture (S.T. Lovett, personal communication).

Protein Lysates, Immunoblots, and *lacZ* Assays

At least three independent cultures were grown to mid-log with or without 100 mM HU for 1 hr. Cultures were lysed by bead beater. Immunoblotting was performed as previously described (Robichon et al., 2005), loading equal amounts of protein lysate for each sample. Relative protein expression levels were quantitated using a FluorChem HD2 Imaging System (Alpha Innotech Corp.) and expressed as the average ± SE. LacZ assays were performed as previously described (Sambrook and Russell, 2001).

Microscopy and Flow Cytometry Analysis

Strains were grown to exponential phase, diluted, and grown for 1 hr with or without 100 mM HU. Preparation of cells for live-cell microscopy was done essentially as described (Godoy et al., 2006). Flow cytometry analysis was performed as described (Dwyer et al., 2007). Flow cytometry experiments measured the entire population of cells, and all plots represent analysis of an equal number of cells ($\geq$ 50,000 cells). The relative fluorescence values were determined by taking the mean fluorescence value for each sample at each time point and normalizing that value to the maximum mean fluorescence value that the wild-type sample achieved over the time course. Each data point represents the average of three independent measurements of these relative fluorescence values, and the error bars represent SE of the independent measurements. Hydroxyl radical formation was measured by 3′-(p-hydroxyphenyl) fluorescein (HPF; Molecular Probes). An example of the side scatter and forward scatter for one experiment measuring HPF fluorescence is shown in Figure S4. Cell death was measured using Propidium Iodide (Molecular Probes). Cell membrane depolarization was monitored using DiBAC4 (Molecular Probes).

SUPPLEMENTAL DATA

Supplemental Data include two tables and three figures and can be found with this article online at http://www.cell.com/molecular-cell/supplemental/S1097-2765(09)00865-X.

REFERENCES

Ades, S.E. (2008). Regulation by destruction: design of the sigmaE envelope stress response. Curr. Opin. Microbiol. *11*, 535–540.

Ahmad, S.I., Kirk, S.H., and Eisenstark, A. (1998). Thymine metabolism and thymineless death in prokaryotes and eukaryotes. Annu. Rev. Microbiol. *52*, 591–625.

Alba, B.M., and Gross, C.A. (2004). Regulation of the Escherichia coli sigma-dependent envelope stress response. Mol. Microbiol. *52*, 613–619.

Barbe, J., Villaverde, A., and Guerrero, R. (1987). Induction of the SOS response by hydroxyurea in Escherichia coli K12. Mutat. Res. *192*, 105–108.

Belevich, I., Borisov, V.B., Konstantinov, A.A., and Verkhovsky, M.I. (2005). Oxygenated complex of cytochrome bd from Escherichia coli: stability and photolability. FEBS Lett. *579*, 4567–4570.

Belevich, I., Borisov, V.B., Bloch, D.A., Konstantinov, A.A., and Verkhovsky, M.I. (2007). Cytochrome bd from Azotobacter vinelandii: evidence for high-affinity oxygen binding. Biochemistry *46*, 11177–11184.

Bolstad, B.M., Irizarry, R.A., Astrand, M., and Speed, T.P. (2003). A comparison of normalization methods for high density oligonucleotide array data based on variance and bias. Bioinformatics *19*, 185–193.

Britton, R.A., Kuster-Schock, E., Auchtung, T.A., and Grossman, A.D. (2007). SOS induction in a subpopulation of structural maintenance of chromosome (Smc) mutant cells in Bacillus subtilis. J. Bacteriol. *189*, 4359–4366.

Buts, L., Lah, J., Dao-Thi, M.H., Wyns, L., and Loris, R. (2005). Toxin-antitoxin modules as bacterial metabolic stress managers. Trends Biochem. Sci. *30*, 672–679.

Christensen, S.K., and Gerdes, K. (2003). RelE toxins from bacteria and Archaea cleave mRNAs on translating ribosomes, which are rescued by tmRNA. Mol. Microbiol. *48*, 1389–1400.

Couturier, M., Bahassi, e.-M., and Van Melderen, L. (1998). Bacterial death by DNA gyrase poisoning. Trends Microbiol. *6*, 269–275.

Dueweke, T.J., and Gennis, R.B. (1991). Proteolysis of the cytochrome d complex with trypsin and chymotrypsin localizes a quinol oxidase domain. Biochemistry *30*, 3401–3406.

Dukan, S., Farewell, A., Ballesteros, M., Taddei, F., Radman, M., and Nystrom, T. (2000). Protein oxidation in response to increased transcriptional or translational errors. Proc. Natl. Acad. Sci. USA *97*, 5746–5749.

Dwyer, D.J., Kohanski, M.A., Hayete, B., and Collins, J.J. (2007). Gyrase inhibitors induce an oxidative damage cellular death pathway in *Escherichia coli*. Mol. Syst. Biol. *3*, 91.

Engelberg-Kulka, H., Amitai, S., Kolodkin-Gal, I., and Hazan, R. (2006). Bacterial programmed cell death and multicellular behavior in bacteria. PLoS Genet. *2*, e135.

Faith, J.J., Hayete, B., Thaden, J.T., Mogno, I., Wierzbowski, J., Cottarel, G., Kasif, S., Collins, J.J., and Gardner, T.S. (2007). Large-Scale Mapping and Validation of Escherichia coli Transcriptional Regulation from a Compendium of Expression Profiles. PLoS Biol. *5*, e8.

Foti, J.J., Schienda, J., Sutera, V.A., Jr., and Lovett, S.T. (2005). A bacterial G protein-mediated response to replication arrest. Mol. Cell *17*, 549–560.

Friedberg, E.C., Walker, G.C., Siede, W., Wood, R.D., Schultz, R.A., and Ellenberger, T. (2005). DNA Repair and Mutagenesis, Second Edition (Washington, DC: ASM Press).

Fuchs, J.A., and Karlstrom, H.O. (1973). A mutant of Escherichia coli defective in ribonucleosidediphosphate reductase. 2. Characterization of the enzymatic defect. Eur. J. Biochem. *32*, 457–462.

Gefter, M.L., Hirota, Y., Kornberg, T., Wechsler, J.A., and Barnoux, C. (1971). Analysis of DNA polymerases II and 3 in mutants of Escherichia coli thermosensitive for DNA synthesis. Proc. Natl. Acad. Sci. USA *68*, 3150–3153.

Gerdes, K., Christensen, S.K., and Lobner-Olesen, A. (2005). Prokaryotic toxin-antitoxin stress response loci. Nat. Rev. Microbiol. *3*, 371–382.

Gibert, I., Calero, S., and Barbe, J. (1990). Measurement of in vivo expression of nrdA and nrdB genes of Escherichia coli by using lacZ gene fusions. Mol. Gen. Genet. *220*, 400–408.

Godoy, V.G., Jarosz, D.F., Walker, F.L., Simmons, L.A., and Walker, G.C. (2006). Y-family DNA polymerases respond to DNA damage-independent inhibition of replication fork progression. EMBO J. *25*, 868–879.

Hayes, F. (2003). Toxins-antitoxins: plasmid maintenance, programmed cell death, and cell cycle arrest. Science *301*, 1496–1499.

Heller, R.C., and Marians, K.J. (2005). The disposition of nascent strands at stalled replication forks dictates the pathway of replisome loading during restart. Mol. Cell *17*, 733–743.

Heller, R.C., and Marians, K.J. (2006). Replication fork reactivation downstream of a blocked nascent leading strand. Nature *439*, 557–562.

Imlay, J.A. (2003). Pathways of oxidative damage. Annu. Rev. Microbiol. *57*, 395–418.

Imlay, J.A., and Fridovich, I. (1991). Superoxide production by respiring membranes of Escherichia coli. Free Radic. Res. Commun. *12-13*, 59–66.

Imlay, J.A., Chin, S.M., and Linn, S. (1988). Toxic DNA damage by hydrogen peroxide through the Fenton reaction in vivo and in vitro. Science *240*, 640–642.

Jakubovics, N.S., and Jenkinson, H.F. (2001). Out of the iron age: new insights into the critical role of manganese homeostasis in bacteria. Microbiology *147*, 1709–1718.

Jensen, R.B., and Gerdes, K. (1995). Programmed cell death in bacteria: proteic plasmid stabilization systems. Mol. Microbiol. *17*, 205–210.

Jepras, R.I., Paul, F.E., Pearson, S.C., and Wilkinson, M.J. (1997). Rapid assessment of antibiotic effects on Escherichia coli by bis-(1,3-dibutylbarbituric acid) trimethine oxonol and flow cytometry. Antimicrob. Agents Chemother. *41*, 2001–2005.

Jones, J., Studholme, D.J., Knight, C.G., and Preston, G.M. (2007). Integrated bioinformatic and phenotypic analysis of RpoN-dependent traits in the plant growth-promoting bacterium Pseudomonas fluorescens SBW25. Environ. Microbiol. *9*, 3046–3064.

Jordan, A., and Reichard, P. (1998). Ribonucleotide reductases. Annu. Rev. Biochem. *67*, 71–98.

Kabir, M.S., Yamashita, D., Koyama, S., Oshima, T., Kurokawa, K., Maeda, M., Tsunedomi, R., Murata, M., Wada, C., Mori, H., and Yamada, M. (2005). Cell lysis directed by sigmaE in early stationary phase and effect of induction of the rpoE gene on global gene expression in Escherichia coli. Microbiology *151*, 2721–2735.

Kohanski, M.A., Dwyer, D.J., Hayete, B., Lawrence, C.A., and Collins, J.J. (2007). A common mechanism of cellular death induced by bactericidal antibiotics. Cell *130*, 797–810.

Kohanski, M.A., Dwyer, D.J., Wierzbowski, J., Cottarel, G., and Collins, J.J. (2008). Mistranslation of membrane proteins and two-component system activation trigger antibiotic-mediated cell death. Cell *135*, 679–690.

Kolodkin-Gal, I., and Engelberg-Kulka, H. (2006). Induction of Escherichia coli chromosomal mazEF by stressful conditions causes an irreversible loss of viability. J. Bacteriol. *188*, 3420–3423.

Kolodkin-Gal, I., and Engelberg-Kulka, H. (2008). The extracellular death factor: physiological and genetic factors influencing its production and response in Escherichia coli. J. Bacteriol. *190*, 3169–3175.

Kolodkin-Gal, I., Hazan, R., Gaathon, A., Carmeli, S., and Engelberg-Kulka, H. (2007). A linear pentapeptide is a quorum-sensing factor required for mazEF-mediated cell death in Escherichia coli. Science *318*, 652–655.

Kolodkin-Gal, I., Sat, B., Keshet, A., and Engelberg-Kulka, H. (2008). The communication factor EDF and the toxin-antitoxin module mazEF determine the mode of action of antibiotics. PLoS Biol. *6*, e319.

Kren, B., and Fuchs, J.A. (1987). Characterization of the ftsB gene as an allele of the nrdB gene in Escherichia coli. J. Bacteriol. *169*, 14–18.

Lenn, T., Leake, M.C., and Mullineaux, C.W. (2008). Clustering and dynamics of cytochrome bd-I complexes in the Escherichia coli plasma membrane in vivo. Mol. Microbiol. *70*, 1397–1407.

Lopes, M., Cotta-Ramusino, C., Pellicioli, A., Liberi, G., Plevani, P., Muzi-Falconi, M., Newlon, C.S., and Foiani, M. (2001). The DNA replication checkpoint response stabilizes stalled replication forks. Nature *412*, 557–561.

Lorence, R.M., and Gennis, R.B. (1989). Spectroscopic and quantitative analysis of the oxygenated and peroxy states of the purified cytochrome d complex of Escherichia coli. J. Biol. Chem. *264*, 7135–7140.

Lovett, S.T. (2005). Filling the gaps in replication restart pathways. Mol. Cell *17*, 751–752.

Ma, X., Ehrhardt, D.W., and Margolin, W. (1996). Colocalization of cell division proteins FtsZ and FtsA to cytoskeletal structures in living Escherichia coli cells by using green fluorescent protein. Proc. Natl. Acad. Sci. USA *93*, 12998–13003.

MacRitchie, D.M., Buelow, D.R., Price, N.L., and Raivio, T.L. (2008). Two-component signaling and gram negative envelope stress response systems. Adv. Exp. Med. Biol. *631*, 80–110.

Magnuson, R.D. (2007). Hypothetical functions of toxin-antitoxin systems. J. Bacteriol. *189*, 6089–6092.

Moore, E.C., and Hurlbert, R.B. (1985). The inhibition of ribonucleoside diphosphate reductase by hydroxyurea, guanazole and pyrazoloimidazole (IMPY). Pharmacol. Ther. *27*, 167–196.

Moore, S.D., and Sauer, R.T. (2005). Ribosome rescue: tmRNA tagging activity and capacity in Escherichia coli. Mol. Microbiol. *58*, 456–466.

Moore, S.D., and Sauer, R.T. (2007). The tmRNA system for translational surveillance and ribosome rescue. Annu. Rev. Biochem. *76*, 101–124.

Mount, D.W., Low, K.B., and Edmiston, S.J. (1972). Dominant mutations (lex) in Escherichia coli K-12 which affect radiation sensitivity and frequency of ultraviolet lght-induced mutations. J. Bacteriol. *112*, 886–893.

Nakayama, K., Kusano, K., Irino, N., and Nakayama, H. (1994). Thymine starvation-induced structural changes in Escherichia coli DNA. Detection by pulsed field gel electrophoresis and evidence for involvement of homologous recombination. J. Mol. Biol. *243*, 611–620.

Novogrodsky, A., Ravid, A., Rubin, A.L., and Stenzel, K.H. (1982). Hydroxyl radical scavengers inhibit lymphocyte mitogenesis. Proc. Natl. Acad. Sci. USA *79*, 1171–1174.

Poole, R.K., and Cook, G.M. (2000). Redundancy of aerobic respiratory chains in bacteria? Routes, reasons and regulation. Adv. Microb. Physiol. *43*, 165–224.

Postle, K., and Larsen, R.A. (2007). TonB-dependent energy transduction between outer and cytoplasmic membranes. Biometals *20*, 453–465.

Repine, J.E., Fox, R.B., and Berger, E.M. (1981). Hydrogen peroxide kills Staphylococcus aureus by reacting with staphylococcal iron to form hydroxyl radical. J. Biol. Chem. *256*, 7094–7096.

Robichon, C., Vidal-Ingigliardi, D., and Pugsley, A.P. (2005). Depletion of apolipoprotein N-acyltransferase causes mislocalization of outer membrane lipoproteins in Escherichia coli. J. Biol. Chem. *280*, 974–983.

Rosenkranz, H.S., Winshell, E.B., Mednis, A., Carr, H.S., and Ellner, C.J. (1967). Studies with hydroxyurea. VII. Hydroxyurea and the synthesis of functional proteins. J. Bacteriol. *94*, 1025–1033.

Ruiz, N., and Silhavy, T.J. (2005). Sensing external stress: watchdogs of the Escherichia coli cell envelope. Curr. Opin. Microbiol. *8*, 122–126.

Saavedra De Bast, M., Mine, N., and Van Melderen, L. (2008). Chromosomal toxin-antitoxin systems may act as antiaddiction modules. J. Bacteriol. *190*, 4603–4609.

Sambrook, J., and Russell, D.W. (2001). Molecular Cloning: A Laboratory Manual, Third Edition (Cold Spring Harbor, NY: Cold Spring Harbor Laboratory Press).

Sat, B., Reches, M., and Engelberg-Kulka, H. (2003). The Escherichia coli mazEF suicide module mediates thymineless death. J. Bacteriol. *185*, 1803–1807.

Schumacher, M.A., Piro, K.M., Xu, W., Hansen, S., Lewis, K., and Brennan, R.G. (2009). Molecular mechanisms of HipA-mediated multidrug tolerance and its neutralization by HipB. Science *323*, 396–401.

Seaver, L.C., and Imlay, J.A. (2001). Alkyl hydroperoxide reductase is the primary scavenger of endogenous hydrogen peroxide in Escherichia coli. J. Bacteriol. *183*, 7173–7181.

Setsukinai, K., Urano, Y., Kakinuma, K., Majima, H.J., and Nagano, T. (2003). Development of novel fluorescence probes that can reliably detect reactive oxygen species and distinguish specific species. J. Biol. Chem. *278*, 3170–3175.

Simmons, L.A., Foti, J.J., Cohen, S.E., and Walker, G.C. (2008a). Escherichia coli and Salmonella: cellular and molecular biology, Vol, Chapter 5.4.3 (Washington, D. C.: ASM Press).

Simmons, L.A., Goranov, A.I., Kobayashi, H., Davies, B.W., Yuan, D.S., Grossman, A.D., and Walker, G.C. (2008b). A comparison of responses to double-strand breaks between Escherichia coli and Bacillus subtilis reveals different requirements for SOS induction. J. Bacteriol. *191*, 1152–1161.

Sinha, N.K., and Snustad, D.P. (1972). Mechanism of inhibition of deoxyribonucleic acid synthesis in Escherichia coli by hydroxyurea. J. Bacteriol. *112*, 1321–1324.

Sjoberg, B.M., Hahne, S., Karlsson, M., Jornvall, H., Goransson, M., and Uhlin, B.E. (1986). Overproduction and purification of the B2 subunit of ribonucleotide reductase from Escherichia coli. J. Biol. Chem. *261*, 5658–5662.

Sneeden, J.L., and Loeb, L.A. (2004). Mutations in the R2 subunit of ribonucleotide reductase that confer resistance to hydroxyurea. J. Biol. Chem. *279*, 40723–40728.

Sogo, J.M., Lopes, M., and Foiani, M. (2002). Fork reversal and ssDNA accumulation at stalled replication forks owing to checkpoint defects. Science *297*, 599–602.

Strauss, B., Kelly, K., and Ekiert, D. (2005). Cytochrome oxidase deficiency protects Escherichia coli from cell death but not from filamentation due to thymine deficiency or DNA polymerase inactivation. J. Bacteriol. *187*, 2827–2835.

Stubbe, J. (2003). Di-iron-tyrosyl radical ribonucleotide reductases. Curr. Opin. Chem. Biol. *7*, 183–188.

Timson, J. (1975). Hydroxyurea. Mutat. Res. *32*, 115–132.

Touati, D., Jacques, M., Tardat, B., Bouchard, L., and Despied, S. (1995). Lethal oxidative damage and mutagenesis are generated by iron in delta fur mutants of Escherichia coli: protective role of superoxide dismutase. J. Bacteriol. *177*, 2305–2314.

Tsilibaris, V., Maenhaut-Michel, G., Mine, N., and Van Melderen, L. (2007). What is the benefit to Escherichia coli of having multiple toxin-antitoxin systems in its genome? J. Bacteriol. *189*, 6101–6108.

Tsubaki, M., Hori, H., and Mogi, T. (2000). Probing molecular structure of dioxygen reduction site of bacterial quinol oxidases through ligand binding to the redox metal centers. J. Inorg. Biochem. *82*, 19–25.

Wandersman, C., and Delepelaire, P. (2004). Bacterial iron sources: from siderophores to hemophores. Annu. Rev. Microbiol. *58*, 611–647.

Wasil, M., Halliwell, B., Grootveld, M., Moorhouse, C.P., Hutchison, D.C., and Baum, H. (1987). The specificity of thiourea, dimethylthiourea and dimethyl sulphoxide as scavengers of hydroxyl radicals. Their protection of alpha 1-antiproteinase against inactivation by hypochlorous acid. Biochem. J. *243*, 867–870.

Weiss, D.S., Chen, J.C., Ghigo, J.M., Boyd, D., and Beckwith, J. (1999). Localization of FtsI (PBP3) to the septal ring requires its membrane anchor, the Z ring, FtsA, FtsQ, and FtsL. J. Bacteriol. *181*, 508–520.

Wickner, W., and Kornberg, A. (1974). A holoenzyme form of deoxyribonucleic acid polymerase III. Isolation and properties. J. Biol. Chem. *249*, 6244–6249.

Wiener, M.C. (2005). TonB-dependent outer membrane transport: going for Baroque? Curr. Opin. Struct. Biol. *15*, 394–400.

Yang, K., Borisov, V.B., Konstantinov, A.A., and Gennis, R.B. (2008). The fully oxidized form of the cytochrome bd quinol oxidase from E. coli does not participate in the catalytic cycle: direct evidence from rapid kinetics studies. FEBS Lett. *582*, 3705–3709.

Zhang, Y., Zhang, J., Hara, H., Kato, I., and Inouye, M. (2005). Insights into the mRNA cleavage mechanism by MazF, an mRNA interferase. J. Biol. Chem. *280*, 3143–3150.